Mon. Not. R. Astron. Soc. **328,** 969–976 (2001)

The fragmentation of pre-enriched primordial objects

V. Bromm,[1,2★] A. Ferrara,[3] P. S. Coppi[2] and R. B. Larson[2]

[1]*Institute of Astronomy, Madingley Road, Cambridge CB3 0HA*
[2]*Department of Astronomy, Yale University, New Haven, CT 06520-8101, USA*
[3]*Osservatorio Astrofisico di Arcetri, Largo E. Fermi 5, 50125 Firenze, Italy*

Accepted 2001 August 20. Received 2001 August 13; in original form 2001 April 25

ABSTRACT

Recent theoretical investigations have suggested that the formation of the very first stars, forming out of metal-free gas, was fundamentally different from the present-day case. The question then arises which effect was responsible for this transition in the star formation properties. In this paper, we study the effect of metallicity on the evolution of the gas in a collapsing dark matter mini-halo. We model such a system as an isolated 3σ peak of mass $2 \times 10^6\,\mathrm{M}_\odot$ that collapses at $z_{\rm coll} \simeq 30$, using smoothed particle hydrodynamics. The gas has a supposed level of pre-enrichment of either $Z = 10^{-4}\,\mathrm{Z}_\odot$ or $10^{-3}\,\mathrm{Z}_\odot$. We assume that H_2 has been radiatively destroyed by the presence of a soft UV background. Metals therefore provide the only viable cooling at temperatures below 10^4 K. We find that the evolution proceeds very differently for the two cases. The gas in the lower metallicity simulation fails to undergo continued collapse and fragmentation, whereas the gas in the higher metallicity case dissipatively settles into the centre of the dark matter halo. The central gas, characterized by densities $n_{\rm H} \gtrsim 10^4\,\mathrm{cm}^{-3}$, and a temperature, $T \simeq 90$ K, that closely follows that of the cosmic microwave background, is gravitationally unstable and undergoes vigorous fragmentation. We discuss the physical reason for the existence of a critical metallicity, $Z_{\rm crit} \sim 5 \times 10^{-4}\,\mathrm{Z}_\odot$, and its possible dependence on redshift. Compared with the pure H/He case, the fragmentation of the $Z = 10^{-3}\,\mathrm{Z}_\odot$ gas leads to a larger relative number of low-mass clumps.

Key words: hydrodynamics – stars: formation – galaxies: formation – cosmology: theory – early Universe.

1 INTRODUCTION

One of the grand challenges in modern astrophysics is to understand how the cosmic 'dark ages' ended, and to elucidate the nature of the first luminous objects (e.g. Rees 1999; Barkana & Loeb 2001). Recently, various authors have addressed the properties of the very first generation of stars through numerical simulations of the collapse and fragmentation of primordial clouds, consisting of dark matter (DM) and metal-free, pure H/He gas (Abel et al. 1998; Bromm, Coppi & Larson 1999, 2001; Nakamura & Umemura 1999; Abel, Bryan & Norman 2000). In the context of hierarchical models of structure formation, these so-called Population III stars are expected to form in haloes of mass $\sim 10^5$–$10^6\,\mathrm{M}_\odot$, collapsing at $z \simeq 20$–30 (Tegmark et al. 1997). The three-dimensional numerical investigations have suggested that Population III stars were rather massive, perhaps even very massive with $M_* \geq 100\,\mathrm{M}_\odot$ (Bromm et al. 1999, 2001; Abel et al. 2000). Based on two-dimensional studies, Nakamura & Umemura (2001) have hypothesized a bimodal initial mass function (IMF) for the first stars, with one mode favouring very massive stars, and the other leading to 'normal' stars of mass $\sim 1\,\mathrm{M}_\odot$. The existence of a high characteristic mass scale has a robust explanation in the microphysics of cooling arising from H_2, which is the main coolant in the absence of metals.

Although important uncertainties remain, mostly deriving from the poorly understood physics of the protostellar feedback, it seems plausible that the formation of Population III stars was qualitatively different from present-day (Population I) star formation. The question, therefore, arises: *How did the transition in the star formation properties take place, and what is the physics responsible for it?* In this paper, we investigate arguably the most important effect: the presence of a trace amount of heavy elements. These metals were likely injected into the gas during a pre-enrichment event, because self-enrichment is rendered highly implausible owing to the blowaway of any remaining gas after the first (Population III) stars have exploded as SNe, given the relatively small binding energy of Population III DM haloes (Ciardi et al. 2000).

★E-mail: volker@ast.cam.ac.uk

© 2001 RAS

Downloaded from https://academic.oup.com/mnras/article/328/3/969/1247014 by Luisa Ferrini user on 02 December 2025

We here consider the limiting case in which all the H_2 has been radiatively destroyed by the presence of a soft UV background. H_2 molecules are very vulnerable to photons with energies below the Lyman limit. Even before the Universe was reionized, a pervasive, soft UV radiation field could therefore have been established (e.g. Ciardi et al. 2000). Metals consequently provide the only cooling at temperatures $T \lesssim 10^4$ K.

Other important roles in modifying the physics of star formation might be attributable to magnetic fields, or to the onset of turbulence. Both these effects are believed to be unimportant in the formation of the very first stars (e.g. Loeb 1998), but it will be interesting to explore their role in forming the second generation of stars in future work.

Previous work on this question has focused on the chemical and thermal history of the gas, employing a simple one-zone model for the dynamical evolution of the collapsing cloud (e.g. Silk 1977; Yoshii & Sabano 1980; Lin & Murray 1992; Nishi & Tashiro 2000; Omukai 2000). Following the collapse to the point where the gas becomes opaque, Omukai (2000) argues that the resulting mass of the protostellar core is independent of metallicity. The final stellar mass, however, is expected to have no direct relation to the initial (core) mass, and is mainly determined by the continued accretion on to the protostellar core. Our approach, based on full three-dimensional numerical simulations of a collapsing primordial cloud, allows for the creation of sink particles and is thus well suited to address the complex physics of accretion.

The paper is organized as follows. In Section 2, we present our numerical methodology. The choice and justification for the initial conditions and the results of the simulation are discussed in Section 3. We summarize our findings, and address their implications in the final section.

2 NUMERICAL METHOD

The evolution of the dark matter and gas components is calculated with a version of TREESPH (Hernquist & Katz 1989), combining the smoothed particle hydrodynamics (SPH) method with a hierarchical (tree) gravity solver (see Bromm et al. 2001 for further details). Here, we discuss the additions to the code that are necessary for the investigation of low-metallicity gas. These are a method to treat the radiative cooling of the gas, and a technique to create sink particles. The thermal evolution of the gas is governed by the equation:

$$\frac{\mathrm{D}u}{\mathrm{D}t} = \frac{P}{\rho^2}\frac{\mathrm{D}\rho}{\mathrm{D}t} + \frac{\Gamma - \Lambda}{\rho}, \tag{1}$$

where $\mathrm{D}/\mathrm{D}t$ is the usual Lagrangian time derivative, P and ρ are the gas pressure and density, u is the specific internal energy (in erg g^{-1}), and Γ and Λ are the contributions from radiative heating and cooling, respectively (in units of erg cm^{-3} s^{-1}). The first term on the right-hand side describes adiabatic cooling resulting from expansion or heating resulting from compression. We now discuss the relevant radiative processes.

We use the cooling function of Ricotti, Ferrara & Miniati (1997), which includes cooling by fine structure and metastable lines of C, N, O, Fe, S and Si. Ionization equilibrium is supposed to be maintained by cosmic rays that we assume to be associated with the heavy-element production by SNe. The (primary) cosmic ray ionization rate is scaled from the Galactic value, $\zeta_{\mathrm{CR}} = 1.8 \times 10^{-17}\,\mathrm{s}^{-1}$ (McKee 1995), by the factor $Z/\mathrm{Z}_\odot$, where $\mathrm{Z}_\odot$ is the solar metallicity. The same scaling with Z is used to derive the dust-to-gas ratio, which we take locally to be equal to 1/160. Again, the rationale is that dust at high redshift can only be formed in the ejecta of primordial Type II SNe (Todini & Ferrara 2001); hence, its production occurs simultaneously with the injection of heavy elements into the intergalactic medium (IGM). Dust, however, is only marginally important for the cooling (via electron recombinations on positively charged grains) at the low heavy-element abundances we are interested in. In Fig. 1, we show the resulting cooling function for two different metallicities.

As radiative cooling to temperatures below that of the cosmic microwave background (CMB), $T_{\mathrm{CMB}} = 2.7\,\mathrm{K}(1+z)$, is thermodynamically not possible, we write for the cooling term

$$\Lambda = \Lambda(T) - \Lambda(T_{\mathrm{CMB}}). \tag{2}$$

For $T < T_{\mathrm{CMB}}$, radiative cooling consequently turns into heating. This approximate treatment ensures that $T \geq T_{\mathrm{CMB}}$, unless cooling proceeds via adiabatic expansion. At $z \gtrsim 30$, gas temperatures are therefore limited to $T \gtrsim 90$ K, justifying the neglect of cooling arising from molecules, such as CO, which would become important only at lower temperatures.

Owing to the assumed complete destruction of H_2 in the presence of a soft UV field, hydrogen molecules do not contribute to the cooling of the gas. Prior to reionization there are almost no ionizing photons, and we consequently ignore heating arising from photo-ionization.

We include heating resulting from the photoelectric effect on dust grains. This is consistent with our assumption that all the H_2 has been destroyed by the presence of a soft UV background, because the photoelectric heating is mostly caused by photons in the same spectral range. We write the heating resulting from the photoelectric effect as $\Gamma = an$, with $a = a_\odot(Z/\mathrm{Z}_\odot)$. For the local value of the heating constant, we choose $a_\odot \simeq 10^{-24}\epsilon\,\mathrm{erg\,s^{-1}}$, with a heating efficiency of $\epsilon \simeq 0.05$ (Wolfire et al. 1995). As we discuss later, this effect is not very important for the evolution of the gas.

We have devised an algorithm to merge SPH particles in high-density regions in order to overcome the otherwise prohibitive time-step limitation, as enforced by the Courant stability criterion. To follow the simulation for a few dynamical times, we allow SPH particles to merge into more massive ones, provided they exceed a predetermined density threshold, $n_{\mathrm{th}} \simeq 10^6\,\mathrm{cm^{-3}}$. More details of the merging algorithm are given in Bromm et al. (2001).

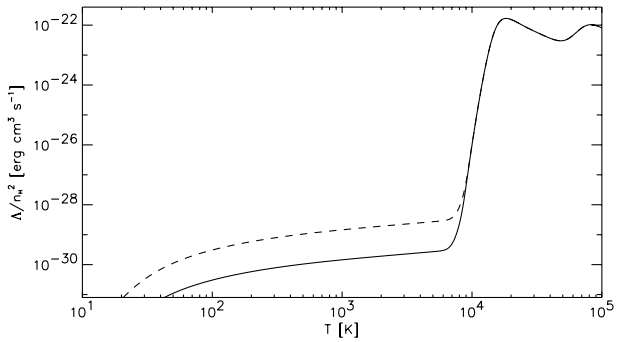

Figure 1. Cooling function for gas that is enriched with a trace amount of metals. Shown is the cooling rate (in units of erg cm^3 s^{-1}) versus temperature, assuming a hydrogen density of $n_{\mathrm{H}} = 1\,\mathrm{cm^{-3}}$. *Solid line:* $Z = 10^{-4}\,\mathrm{Z}_\odot$. *Dashed line:* $Z = 10^{-3}\,\mathrm{Z}_\odot$.

Downloaded from https://academic.oup.com/mnras/article/328/3/969/1247014 by Luisa Ferrini user on 02 December 2025

3 THE SIMULATIONS

3.1 Initial conditions

Within a hierarchical cosmogony, the very first stars are expected to form out of $3-4\sigma$ peaks in the random field of primordial density fluctuations. The early (linear) evolution of such a peak, assumed to be an isolated and roughly spherical overdensity, can be described by the top-hat model (e.g. Padmanabhan 1993). We use the top-hat approximation to specify the initial DM configuration, where we choose the background universe to be described by the critical Einstein–de Sitter (EdS) solution with density parameters $\Omega_{\rm DM}=0.95$, $\Omega_{\rm B}=0.05$, and Hubble constant $h=H_0/(100\,{\rm km\,s^{-1}\,Mpc^{-1}})=0.5$. In this paper, we investigate the fate of a 3σ peak of total mass $2\times10^6\,{\rm M}_\odot$, corresponding to $10^5\,{\rm M}_\odot$ in baryons, which is close to the cosmological Jeans mass (Couchman & Rees 1986). On this mass scale, the standard cold dark matter (CDM) scenario predicts a present-day rms overdensity of $\sigma_0(M)\simeq16$, with a normalization $\sigma_8=1$ on the $8\,h^{-1}\,{\rm Mpc}$ scale. Then, one can estimate the redshift of collapse (or virialization) from $1+z_{\rm coll}=3\sigma_0(M)/1.69$, leading to $z_{\rm coll}\simeq30$.

Recent observations (see Barkana & Loeb 2001 and references therein) have presented evidence for a flat universe with $\Omega_{\rm m}=1-\Omega_\Lambda=0.3$, thus rendering the EdS universe increasingly implausible. At high redshifts ($z\gtrsim10$), however, the standard CDM model deviates only slightly from the more realistic ΛCDM case, and serves as a useful template for all hierarchical models of structure formation. The results presented in this paper mainly rely on the cooling physics of the gaseous component, and are not likely to change significantly, if these more realistic cosmological parameters are adopted.

Our simulation is initialized at $z_{\rm i}=100$, by performing the following steps. The collisionless DM particles are placed on a cubical Cartesian grid, and are then perturbed according to a given power spectrum $P(k)=Ak^n$, by applying the Zeldovich approximation (Zeldovich 1970), which also allows us to assign initial velocities self-consistently. The power-law index is set to $n=-3$, which is the asymptotic small-scale behaviour in the standard CDM model (Peebles 1993). To fix the amplitude A, we specify the initial variance of the fluctuations

$$\sigma_{\rm i}^2=A\sum k^n. \tag{3}$$

The summation is over all contributing modes, where the minimum wavenumber is given by the overall size of the Cartesian box, and $k_{\rm max}$ by the Nyquist frequency. Choosing $\sigma_{\rm i}^2\simeq0.1$, the rms fluctuation at the moment of collapse is

$$\sigma(z=30)=\left(\frac{1+z_{\rm i}}{1+z}\right)\sigma_{\rm i}\simeq1. \tag{4}$$

This choice ensures that the substructure develops on a similar time-scale to the overall collapse of the background medium. Next, particles within a (proper) radius of $R_{\rm i}=150\,{\rm pc}$ are selected for the simulation. The resulting number of DM particles is here $N_{\rm DM}=14\,123$. Finally, the particles are set into rigid rotation and are endowed with a uniform Hubble expansion (see also Katz 1991). Angular momentum is added by assuming a spin-parameter $\lambda=L|E|^{1/2}/(GM^{5/2})=0.05$, where L, E and M are the total angular momentum, energy and mass, respectively.

The collisional SPH particles ($N_{\rm SPH}=65\,536$) are randomly placed to approximate a uniform initial density. The random sampling inevitably introduces shot-noise. The DM particles were set up on a regular grid specifically to avoid the unphysical shot-noise distribution, which could mask the desired physical power spectrum. For the gas, however, the presence of the shot noise is not a big problem, because the gas mass is initially slightly smaller than the Jeans mass. Therefore, sound waves will efficiently wipe out all initial density disturbances. The SPH particles are endowed with the same Hubble expansion and rigid rotation as the DM ones. For the initial gas temperature, we adopt the value (see Tegmark et al. 1997) $T_{\rm gas,i}\simeq200\,{\rm K}$.

We carry out two simulations: run A having a metallicity of $Z=10^{-3}\,{\rm Z}_\odot$, and run B with one of $Z=10^{-4}\,{\rm Z}_\odot$. These two values bracket those derived from QSO absorption-line studies of the low column density Lyα forest at $z\sim3$ (Pettini 1999). They are also close to those expected to be associated with the reionization process. Otherwise, the two runs have identical initial conditions.

3.2 Results

The evolution of the collapsing clouds separates into two distinct stages. Leading up to the virialization of the DM, the two simulations behave very similarly, and the evolution is rather insensitive to metallicity. Once the gas has reached a roughly pressure-supported state in the potential of the DM halo, the subsequent evolution bifurcates, resulting in continued collapse and fragmentation for Run A, and in failure to do so for Run B. We now discuss these two stages in turn.

3.2.1 Virialization of dark matter halo

In response to the initially imprinted density fluctuations, the DM develops a marked substructure. The gas does not 'feel' the potential wells of these subcondensations, however, because it cannot cool sufficiently during these early evolutionary phase. Instead, owing to adiabatic compression, $T\propto n^{2/3}$, the gas reaches temperatures of $\sim10^4\,{\rm K}$. At this point, very efficient cooling resulting from the excitation of hydrogen lines sets in (see Fig. 1), and maintains the gas at this temperature upon further compression. At the end of the virialization process, the gas has reached a state of rough pressure support with typical gas temperatures close to the virial temperature,

$$T_{\rm vir}=\frac{GMm_{\rm H}}{2k_{\rm B}R_{\rm vir}}\sim5000\,{\rm K}, \tag{5}$$

where $R_{\rm vir}\simeq100\,{\rm pc}$ is the virial radius, G is Newton's constant, $k_{\rm B}$ Boltzmann's constant, and $m_{\rm H}$ the mass of a hydrogen atom. To estimate the corresponding gas density, $n_{\rm vir}$, we consider the baryonic Jeans mass,

$$M_{\rm J}=3\times10^7\,{\rm M}_\odot\left(\frac{T}{5000\,{\rm K}}\right)^{3/2}\left(\frac{n_{\rm H}}{1\,{\rm cm^{-3}}}\right)^{-1/2}, \tag{6}$$

and assume that it has to be approximately equal to the total mass of the halo. Here, $n_{\rm H}$ denotes the hydrogen number density. From imposing $M_{\rm J}\sim2\times10^6\,{\rm M}_\odot$, one then finds $n_{\rm vir}\simeq10^{2.5}\,{\rm cm^{-3}}$. Heating resulting from the photoelectric effect is never important, neither during virialization, nor during the later, baryon-dominated stages. From here on, the further evolution strongly depends on the level of trace metal enrichment.

3.2.2 Further collapse and fragmentation of the gas

We first discuss Run A. Cooling in this case is efficient enough to

Downloaded from https://academic.oup.com/mnras/article/328/3/969/1247014 by Luisa Ferrini user on 02 December 2025

allow further collapse. In Fig. 2, we show the gas morphology and the corresponding thermodynamic state at $z = 30.5$. As can be seen, the gas has dissipatively settled into a disc-like central configuration. This disc is horizontally supported by rotation. In the presence of a DM halo, one expects a contraction by a factor of $1/\lambda \simeq 20$ for rotational support. The size of the disc, as shown in Fig. 2, is in good agreement with this prediction. It is also evident that the disc is subject to a bar-mode ($m = 2$) instability. By examining the T–$n_{\rm H}$ plane (lower left panel in Fig. 2), one can see that the gas cools efficiently from $\sim 10^4$ K down to the value set by the CMB floor, $T_{\rm min} \simeq T_{\rm CMB} = 86$ K. During this rapid cooling, the gas remains rather smooth. The gravitationally unstable disc-material, however, subsequently undergoes vigorous fragmentation (see Fig. 3).

We next turn to Run B, and to its rather different fate. In Fig. 4, we show the situation at $z \simeq 28$. In contrast to the corresponding situation for Run A (Fig. 3), no further collapse and no fragmentation has occurred. Instead, the gas remains in pressure support, and lingers at temperatures close to $T_{\rm vir}$. Only much later, as the result of slow but inexorable residual cooling, do two high-density clumps form at the very centre of the roughly spherical gas configuration (see Fig. 5). Run B, therefore, presents an example of what Ciardi et al. (2000) have termed a 'dark object', a halo that has failed to produce anything luminous in it.

To summarize, in Run A the gas becomes effectively self-gravitating, leading to continued collapse and fragmentation, whereas in Run B the gas does not. To see this more clearly, we compare in Fig. 6 the cooling time-scale, $t_{\rm cool} \simeq (n_{\rm H} k_{\rm B} T)/\Lambda$, with the free-fall time, $t_{\rm ff} \simeq (G m_{\rm H} n_{\rm H})^{-1/2}$ (Rees & Ostriker 1977). Whether the gas can reach higher densities because of its self-gravity is decided at the end of the DM virialization process, with the gas having $T \sim 5000$ K and $n_{\rm H} \sim 10^{2.5}$ cm^{-3}. For these values, one has $t_{\rm cool} \simeq t_{\rm ff}$ for Run A, and $t_{\rm cool} > t_{\rm ff}$ for Run B. Consequently, the gas in Run B is not able to cool any further and to reach higher densities.

We now give an analytical estimate for the value of the critical metallicity, $Z_{\rm crit}$, which discriminates between the two cases discussed above. Evaluating the cooling function (see Fig. 1) at $T = 5000$ K, we have

$$\Lambda(Z) \simeq 3 \times 10^{-30}\,{\rm erg\,cm^{-3}\,s^{-1}} \left(\frac{Z}{10^{-4}\,{\rm Z_\odot}}\right) \left(\frac{n_{\rm H}}{1\,{\rm cm^{-3}}}\right)^2. \quad (7)$$

The adiabatic heating, $\Gamma_{\rm ad} = \frac{P}{\rho}\frac{{\rm D}\rho}{{\rm D}t} \simeq \frac{P}{t_{\rm ff}}$, can be written as

$$\Gamma_{\rm ad} \simeq 10^{-24}\,{\rm erg\,cm^{-3}\,s^{-1}} \left(\frac{T}{5000\,{\rm K}}\right) \left(\frac{n_{\rm H}}{300\,{\rm cm^{-3}}}\right)^{3/2}. \quad (8)$$

Equating the two terms yields $Z_{\rm crit} \simeq 5 \times 10^{-4}\,{\rm Z_\odot}$, in accordance with the results of our simulations.

We finally address the dependence of $Z_{\rm crit}$ on the redshift of collapse, $z_{\rm coll}$, and the total mass of the halo, M. The gas temperature and density at the end of the DM virialization are expected to obey the relations $T \sim T_{\rm vir} \propto M^{2/3}(1 + z_{\rm coll})$ and $n_{\rm H} \propto \rho_{\rm vir} \propto (1 + z_{\rm coll})^3$, respectively (e.g. Padmanabhan 1993). Assuming $\Lambda \propto T^{1/2}$ for $10^2 \lesssim T \lesssim 10^4$ K, inserting the virial relations into equations (7) and (8), and normalizing to the case treated in this paper, one approximately finds

$$Z_{\rm crit} \simeq 5 \times 10^{-4}\,{\rm Z_\odot} \left(\frac{M}{2 \times 10^6\,{\rm M_\odot}}\right)^{1/3} \left(\frac{1 + z_{\rm coll}}{31}\right)^{-1}. \quad (9)$$

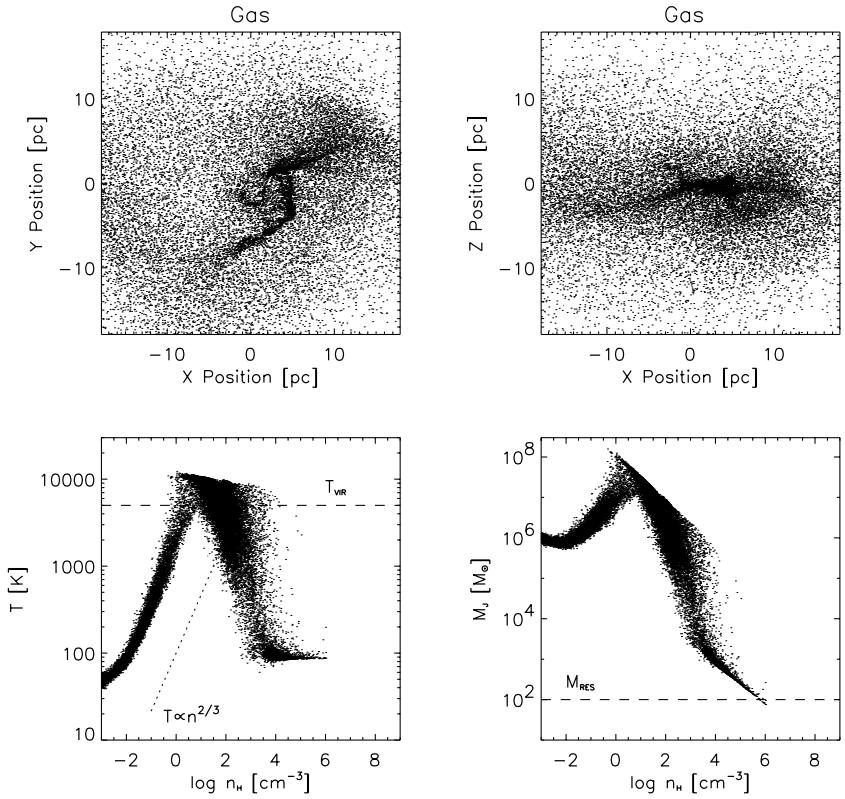

Figure 2. Run A: morphology and gas properties at $z = 30.5$. Top row: the remaining gas in the diffuse phase. Left panels: face-on view. Right panels: edge-on view. The size of the box is 30 pc. It can be seen that the gas has dissipatively settled into a central, disc-like configuration. Lower-left panel: temperature versus hydrogen number density. Lower-right panel: Jeans mass (in units of $M_\odot$) versus hydrogen number density (in units of cm^{-3}).

Downloaded from https://academic.oup.com/mnras/article/328/3/969/1247014 by Luisa Ferrini user on 02 December 2025

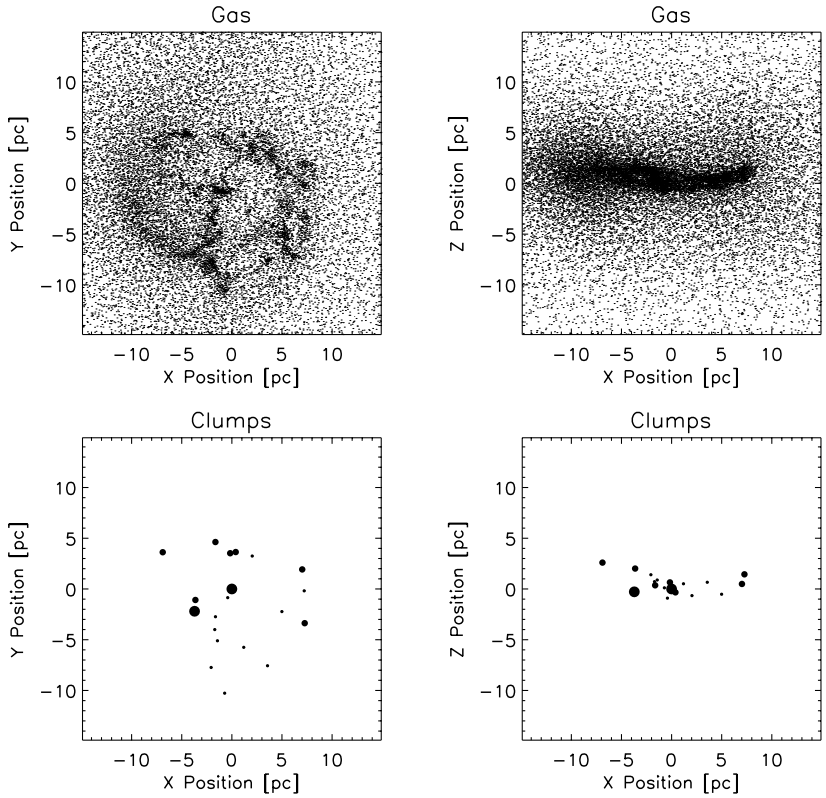

Figure 3. Run A: morphology at $z = 28$. Top row: the remaining gas in the diffuse phase. Bottom row: distribution of clumps. Dot sizes are proportional to the mass of the clumps. Left panels: face-on view. Right panels: edge-on view. The size of the box is 30 pc. It can be seen that the gas has undergone vigorous fragmentation.

This relation is only valid for haloes with $T_{\rm vir} < 10^4$ K. We plan to test this analytical prediction with future simulations.

3.2.3 *Comparison with the Z = 0 case*

Since Bromm et al. (1999, 2001) have investigated the case of zero-metallicity gas with initial conditions that are otherwise very similar to those adopted here, it is instructive to compare our $Z = 10^{-3}\,{\rm Z}_\odot$ simulation with the pure H/He case. In the previous papers, the formation of H_2 was allowed for, whereas here we have considered the limiting case of maximum negative feedback which is supposed to destroy all H_2.

The first difference occurs during the virialization of the DM. In marked contrast to the simulations presented in this paper, the DM fluctuations do imprint their signature on to the gaseous component if H_2 is the main coolant. These DM-induced condensations act as the seeds for the subsequent fragmentation of the gas. The basic reason for this difference is the boost in the formation of H_2 arising from the density and temperature enhancement in the DM subcondensations. Such a chemistry-related feedback is absent in the $Z = 10^{-3}\,{\rm Z}_\odot$ case.

The second, crucial, difference derives from the fact that cooling remains efficient at densities $n_{\rm H} \gtrsim 10^4\,{\rm cm}^{-3}$, provided the gas has been enriched to $Z \geq Z_{\rm crit}$. As can be seen in Fig. 2 (lower-left panel), the gas evolves isothermally up to the threshold density of $n_{\rm th} = 10^6\,{\rm cm}^{-3}$. H_2 cooling, on the other hand, saturates at $n_{\rm H} \gtrsim n_{\rm crit} \simeq 10^3$–$10^4\,{\rm cm}^{-3}$, where $n_{\rm crit}$ marks the transition from NLTE to LTE level populations. By comparing the distribution of $M_{\rm J}$ versus $n_{\rm H}$ in Fig. 2 (lower right panel) with the equivalent fig. 3 (panel (c) in Bromm et al. (1999), it can be seen that there is no characteristic mass scale in the $Z = 10^{-3}\,{\rm Z}_\odot$ case. Such a characteristic scale would correspond to a pile-up of SPH particles in the diagram owing to long evolutionary time-scales. In the pure H/He case, on the other hand, there is a preferred mass scale of $M \sim 10^3\,{\rm M}_\odot$.

The overall range of clump masses, $10^2 < M_{\rm Cl} < 10^4\,{\rm M}_\odot$, is similar in the pure H/He and $Z = 10^{-3}\,{\rm Z}_\odot$ simulations, although the relative number of low-mass clumps is significantly higher for the pre-enriched case. These low-mass clumps have masses close to the resolution limit of the simulation (Bate & Burkert 1997),

$$M_{\rm res} \simeq M_{\rm B}\left(\frac{2N_{\rm neigh}}{N_{\rm SPH}}\right) \simeq 100\,{\rm M}_\odot, \tag{10}$$

where $N_{\rm neigh} \simeq 32$ denotes the number of SPH particles within a smoothing kernel. Obviously, clumps cannot have masses smaller than $M_{\rm res}$. The most massive clumps form with initial masses close to the Jeans mass, $M_{\rm J} \sim 750\,{\rm M}_\odot$, evaluated at the density $n_{\rm H} \simeq 10^4\,{\rm cm}^{-3}$, where the bulk of the freely falling gas reaches the CMB temperature floor, $T_{\rm min} \simeq 86$ K (see Fig. 2).

Later on, clumps gain in mass through accretion from surrounding gas, and through occasional mergers with other clumps. An investigation of the possible subfragmentation of a clump lies beyond the resolution limit of our simulation. It is worth emphasizing that the spectrum of clumps is different from the *stellar* spectrum (i.e. the IMF), and it is not possible to directly derive the latter from the former. However, the qualitative trend that the relative number of low-mass clumps increases with metallicity is suggestive of the possible regulation of the IMF by the gas metal enrichment. To constrain the clump mass spectrum,

Downloaded from https://academic.oup.com/mnras/article/328/3/969/1247014 by Luisa Ferrini user on 02 December 2025

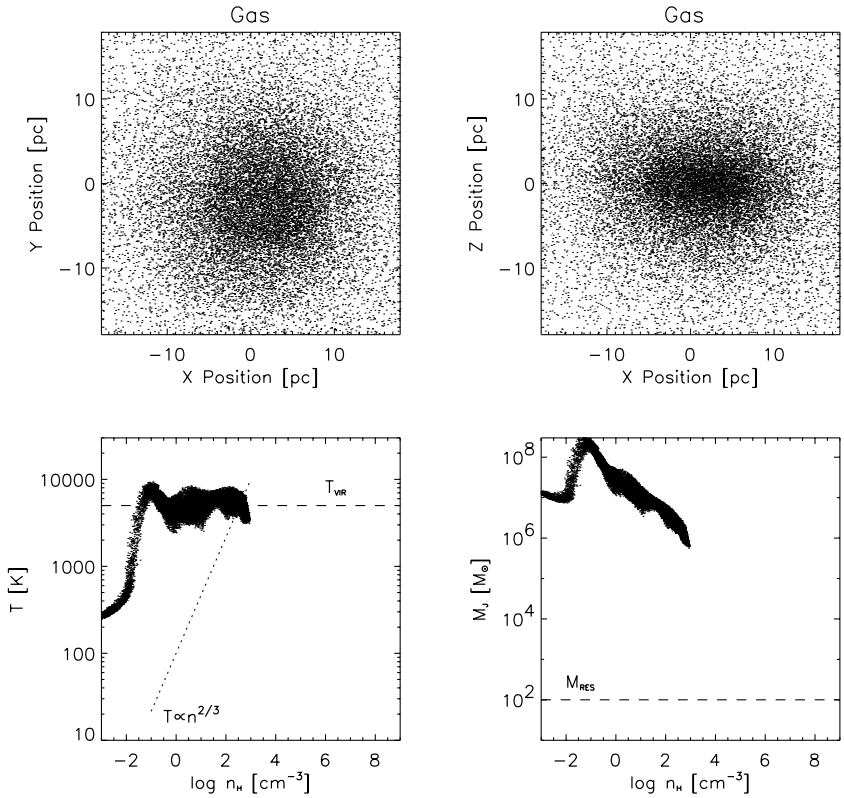

Figure 4. Run B: morphology and thermodynamic properties of the gas at $z = 28$. The convention of Fig. 2 is adopted for the rows and columns.

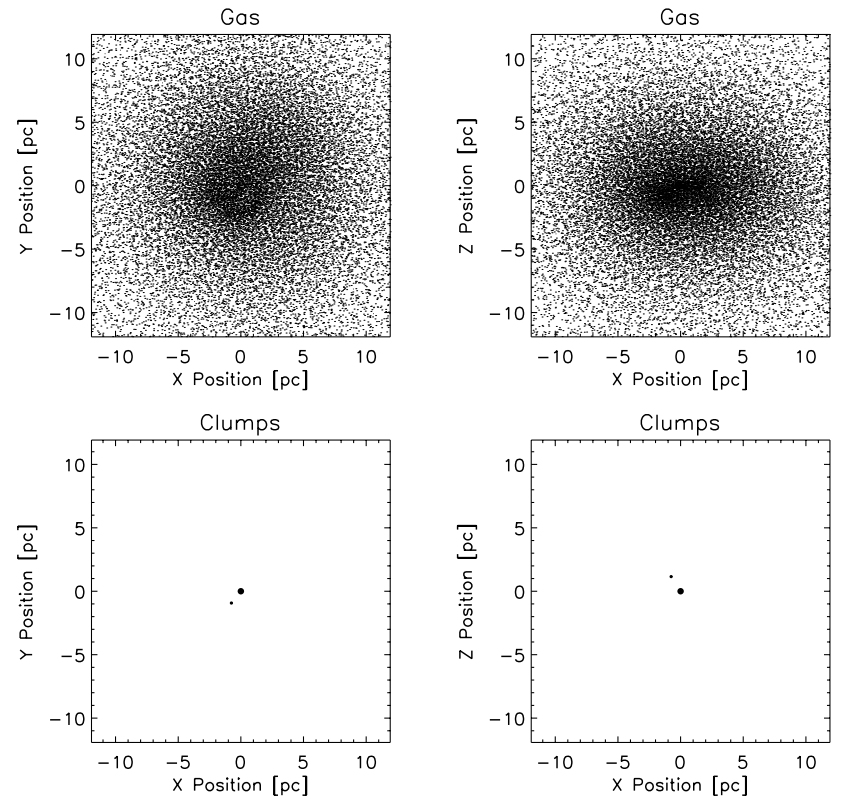

Figure 5. Run B: morphology at $z = 22.7$. The convention of Fig. 3 is adopted for the rows and columns.

Downloaded from https://academic.oup.com/mnras/article/328/3/969/1247014 by Luisa Ferrini user on 02 December 2025

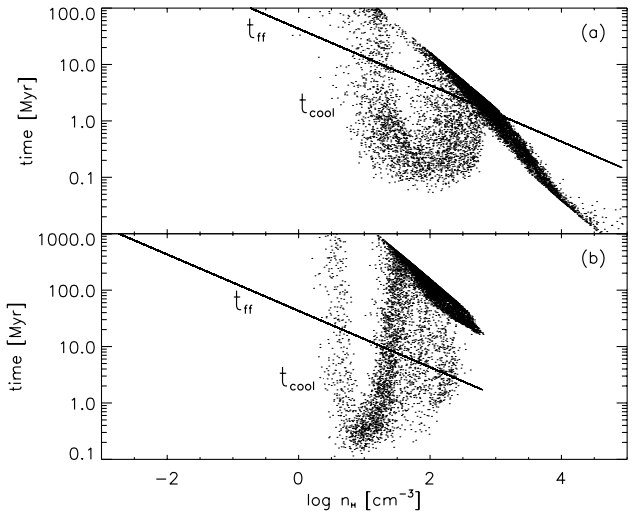

Figure 6. The criterion for continued collapse. Freefall time-scale (solid line) and cooling time-scale (dotted symbols) versus hydrogen number density (in cm^{-3}). Time-scales are in units of 10^6 yr. Shown is the situation briefly after the virialization of the DM, at $z \simeq 30.5$. (a) Run A: the cloud succeeds in undergoing continued collapse owing to efficient cooling, $t_{cool} \sim t_{ff}$, at $\log n_H \simeq 2.5$. (b) Run B: here, $t_{cool} > t_{ff}$ at $\log n_H \simeq 2.5$, and the gas fails to undergo continued collapse.

and eventually the stellar IMF, further, higher resolution studies will be necessary.

The fact that the minimum temperature enforced by the CMB could imply larger Jeans masses at high redshift has already been pointed out by Larson (1998). The role of the CMB in setting the minimum temperature points to the possible importance of z_{coll} in setting an evolving mass scale for cosmic star formation (see Bromm & Clarke 2001 for a discussion of this effect).

4 SUMMARY AND CONCLUSIONS

We have discussed the evolution of primordial star-forming objects in the context of the standard CDM model for structure formation. The studied clouds are pre-enriched to a level of 10^{-4} and $10^{-3}\,Z_\odot$, consistent with observations of the IGM, and collapse close to $z_{coll} \sim 30$. We find that the evolution proceeds very differently in the two cases. The gas in the higher metallicity run can cool efficiently, and consequently collapse to a disc-like configuration. The disc material is gravitationally unstable and fragments into a large number (~ 25) of high-density clumps. In marked contrast to this case, the gas in the lower metallicity simulation cannot cool efficiently, and therefore remains in the post-virialization, pressure-supported state in a roughly spherical configuration. Such a system constitutes an example of a 'dark object', as discussed by Ciardi et al. (2000). These results indicate the existence of a critical metallicity, $Z_{crit} \simeq 5 \times 10^{-4}\,Z_\odot$, below which the presence of heavy elements does not significantly influence the evolution of a primordial cloud. The value of the critical metallicity might be parameter-dependent, being larger at lower z and in more massive haloes. To account for the observed abundance pattern in metal-poor stars, Wasserburg & Qian (2000) have hypothesized an initial, prompt enrichment episode arising from a generation of very massive stars. According to their model, these stars would have formed in gas with [Fe/H] $\lesssim -3$. This nucleosynthetic evidence for a critical metallicity is consistent with our result, which is based on the physics of star formation.

Our investigation has treated the case of a low-mass halo, of mass $\sim 10^6\,M_\odot$, and the question naturally arises of what happens in more massive ones. Is there still a critical metallicity, and if so, what would be its numerical value? In addressing these questions, one can argue that haloes with virial temperatures in excess of $\sim 10^4$ K are much less dependent on a level of pre-enrichment in order to form stars. The gas in these haloes can initially cool through line-excitation of atomic hydrogen, and in the later stages of molecular hydrogen. Even if not present initially, or if completely destroyed in the shocks associated with the virialization process, H_2 is expected to be efficiently formed in the post-shock regions of these systems (e.g. Shapiro & Kang 1987). Owing to their larger binding energy, these haloes can experience multiple episodes of self-enrichment. Whether there is a strong change in the star formation properties, once this internal enrichment exceeds a certain value, cannot be answered without simulating the evolution of such a high-T_{vir} halo.

Although there remain important uncertainties with regard to our findings, we conclude by discussing their potential implications. If indeed stars which formed from extremely low metallicity gas, with $Z < Z_{crit}$, were predominantly massive, this would entail short stellar-evolutionary time-scales, $t_{evol} \sim 10^6$ yr. Consequently, it is not expected to find any extremely low-metallicity stars which are still 'alive' today. This prediction is consistent with observations of metal-poor halo stars, having $Z \geq 10^{-4}\,Z_\odot$ (Beers 2000). Assuming that massive Population III stars end their lives in massive black holes (MBHs), with typical mass $\sim 10^3\,M_\odot$, Madau & Rees (2001) have identified high-σ peaks of mass $\sim 10^6\,M_\odot$, collapsing at $z \simeq 20$–30, as the sites of their formation. As is suggested in this paper, MBHs could only have formed early in the history of the Universe, out of gas with $Z < Z_{crit}$.

If stars more massive than $\sim 250\,M_\odot$ buried their metal production in collapsing to a black hole (Fryer, Woosley & Heger 2001), how did the IGM get enriched to a level of $Z > Z_{crit}$, enabling the subsequent formation of 'normal', low-mass stars? The answer to this question has to await the precise determination of whether the majority of Population III stars has masses below or above the threshold mass for the complete collapse into a black hole, and a better understanding of how the metals are expelled from the star-forming halo (e.g. Madau, Ferrara & Rees 2001).

ACKNOWLEDGMENTS

We thank Lars Hernquist for making available to us a version of TREESPH. Support from the NASA ATP grant NAG5-7074 is gratefully acknowledged. VB thanks the Osservatorio di Arcetri for its hospitality during the completion of this work. This work has been partially supported by the EC RTN network 'The Physics of the Intergalactic Medium'.

REFERENCES

Abel T., Anninos P., Norman M. L., Zhang Y., 1998, ApJ, 508, 518
Abel T., Bryan G. L., Norman M. L., 2000, ApJ, 540, 39
Barkana R., Loeb A., 2001, Phys. Rep., 349, 125
Bate M. R., Burkert A., 1997, MNRAS, 288, 1060
Beers T. C., 2000, in Weiss A., Abel T., Hill V., eds, ESO Astrophys. Symp., The First Stars. Springer, Berlin, p. 3
Bromm V., Clarke C. J., 2001, MNRAS, submitted
Bromm V., Coppi P. S., Larson R. B., 1999, ApJ, 527, L5

Downloaded from https://academic.oup.com/mnras/article/328/3/969/1247014 by Luisa Ferrini user on 02 December 2025

Bromm V., Coppi P. S., Larson R. B., 2001, ApJ, in press (astro-ph/0102503)
Ciardi B., Ferrara A., Governato F., Jenkins A., 2000, MNRAS, 314, 611
Couchman H. M. P., Rees M. J., 1986, MNRAS, 221, 53
Fryer C. L., Woosley S. E., Heger A., 2001, ApJ, 550, 372
Hernquist L., Katz N., 1989, ApJS, 70, 419
Katz N., 1991, ApJ, 368, 325
Larson R. B., 1998, MNRAS, 301, 569
Lin D. N. C., Murray S. D., 1992, ApJ, 394, 523
Loeb A., 1998, in Smith E., Koratkar A., eds, ASP Conf. Ser. Vol. 133, Science with the Next Generation Space Telescope. Astron. Soc. Pac., San Francisco, p. 73
McKee C. F., 1995, in Ferrara A., McKee C. F., Heiles C., Shapiro P. R., eds, ASP Conf. Ser. Vol. 80, The Physics of the Interstellar Medium and Intergalactic Medium. Astron. Soc. Pac., San Francisco, p. 292
Madau P., Rees M. J., 2001, ApJ, 551, L27
Madau P., Ferrara A., Rees M. J., 2001, ApJ, 555, 92
Nakamura F., Umemura M., 1999, ApJ, 515, 239
Nakamura F., Umemura M., 2001, ApJ, 548, 19
Nishi R., Tashiro M., 2000, ApJ, 537, 50
Omukai K., 2000, ApJ, 534, 809
Padmanabhan T., 1993, Structure Formation in the Universe. Cambridge Univ. Press, Cambridge
Peebles P. J. E., 1993, Principles of Physical Cosmology. Princeton Univ. Press, Princeton
Pettini M., 1999, in Walsh J. R., Rosa M. R., eds, ESO Astrophys. Symp., Chemical Evolution from Zero to High Redshift. Springer, Berlin, p. 233
Rees M. J., 1999, in Holt S. S., Smith E., eds, AIP Conf. Proc. 470, After the Dark Ages: When Galaxies Were Young (the Universe at $2 < z < 5$).. Am. Inst. Phys., Woodbury, p. 13
Rees M. J., Ostriker J. P., 1977, MNRAS, 179, 541
Ricotti M., Ferrara A., Miniati F., 1997, ApJ, 485, 254
Shapiro P. R., Kang H., 1987, ApJ, 318, 32
Silk J., 1977, ApJ, 211, 638
Tegmark M., Silk J., Rees M. J., Blanchard A., Abel T., Palla F., 1997, ApJ, 474, 1
Todini P., Ferrara A., 2001, MNRAS, 325, 726
Wasserburg G. J., Qian Y.-Z., 2000, ApJ, 529, L21
Wolfire M. G., Hollenbach D., McKee C. F., Tielens A. G. G. M., Bakes E. L. O., 1995, ApJ, 443, 152
Yoshii Y., Sabano Y., 1980, PASJ, 32, 229
Zeldovich Y. B., 1970, A&A, 5, 84

This paper has been typeset from a TEX/LATEX file prepared by the author.

Downloaded from https://academic.oup.com/mnras/article/328/3/969/1247014 by Luisa Ferrini user on 02 December 2025